Electronic Supplementary Material (ESI) for RSC Advances.

Supporting Information

Selective Chromo-fluorogenic molecular sensor for dual channel recognition of Cu^{2+} and F^{-}: Effect of functional group on selectivity

Soumen Ghosh[a], Aniruddha Ganguly[a], Arghadeep Bhattacharyya[a], Md. Akhtarul Alam[b]*, and Nikhil Guchhait[a]*

[a]Department of Chemistry

University of Calcutta

92, A.P.C. Road, Kolkata 700 009, India

Telephone 91-33-23508386

Fax: 91-33-23519755

[b]Department of Chemistry

Aliah University

IIA/27, New Town, Kolkata-700 156, West Bengal, India

*Corresponding author, E-mail: alam_iitg@yahoo.com (M. A. A.)

and

nguchhait@yahoo.com (N.G.)

Table of Contents

1. Synthesis

1.1. Syntheses and characterization

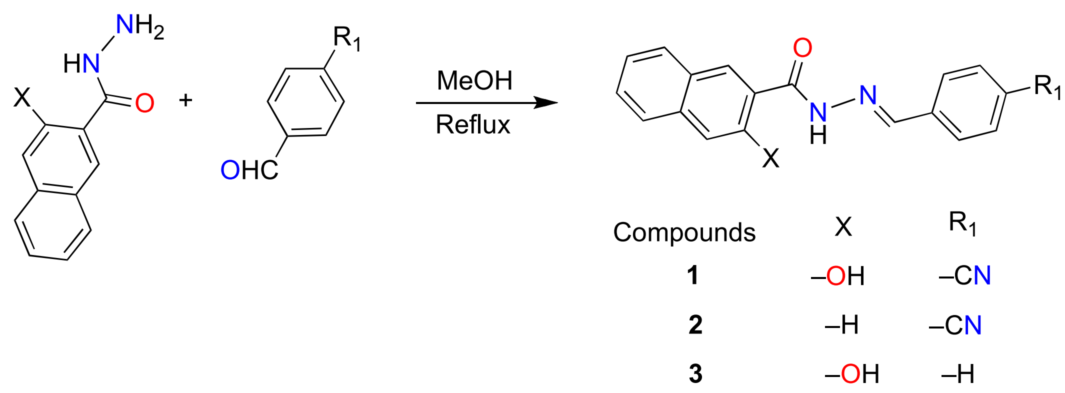

Scheme S1. Syntheses of Compounds **1 (HNHCB)**, **2 (NHCB)**, and **3(HNHB)**

1.2. Compound 2. Sythesis of *naphthalene-2-carboxylic acid (4-cyano-benzylidene)-hydrazide (***NHCB)***:*

Compound **2** has been prepared according to the similar procedure as compound **1** by the reaction between naphthalene-2-carboxylic acid hydrazide (1.3 mmol, 0.250 g) and 4-formyl benzonitrile (1.4 mmol, 0.180 g) in methanol. The colourless solid thus obtained was filtered and then dried under vacuum (yield: 0.32 g, 80%). ^{1}H NMR in d_6-DMSO, 300MHz, δ (ppm): 12.32 (s, 1H, –CONH–), 8.70 (s, 2H, –CH=N– and naph), 8.10-7.96 (m, 8H), 7.68-7.66 (m, 2H), ^{13}C NMR (75.5 MHz, d_6-DMSO, 20 ºC) δ (ppm): 111.00, 120.74, 124.22, 126.26, 127.21, 128.74, 129.08, 129.29, 130.07, 134.58, 136.27, 148.95, 154.51, 164.23, 176. IR (KBr): 3390, 3203, 3055, 2860, 2227, 1655, 1637, 1623, 1571, 1503, 1370, 1300, 1238, 1203, 1071 cm^{-1}.

1.3. Compound 3. Sythesis of *benzylidene 3-hydroxy-naphthalene-2-carbohydrazide*(**HNHCB)***:*

Compound **3** has been also prepared according to the similar procedure as compound **1** by the condensation between 3-hydroxy-naphthalene-2-carboxylic acid hydrazide and benzaldehyde (yield: 72%). ^{1}H NMR in d_6-DMSO, 300MHz, δ (ppm): 12.02 (s, 1H, –CONH–), ~11.5 (broad, 1H, –OH), 8.48 (s, 2H, –CH=N– and naph), 7.94 (d, J=7.8Hz, 1H), 7.80-7.35 (m, 9H). ^{13}C NMR (75.5 MHz, d_6-DMSO, 20 ºC) δ (ppm): 111.04, 116.88, 117.63, 119.06, 119.90, 126.28, 129.08, 129.79, 129.91, 130.74, 132.03, 136.81, 154.50, 157.95, 164.20. IR (KBr): 3242, 3023, 2894, 1659, 1622, 1537, 1487, 1397, 1228, 1213, 1075, 1102, 1070 cm^{-1}.

2. Characterization

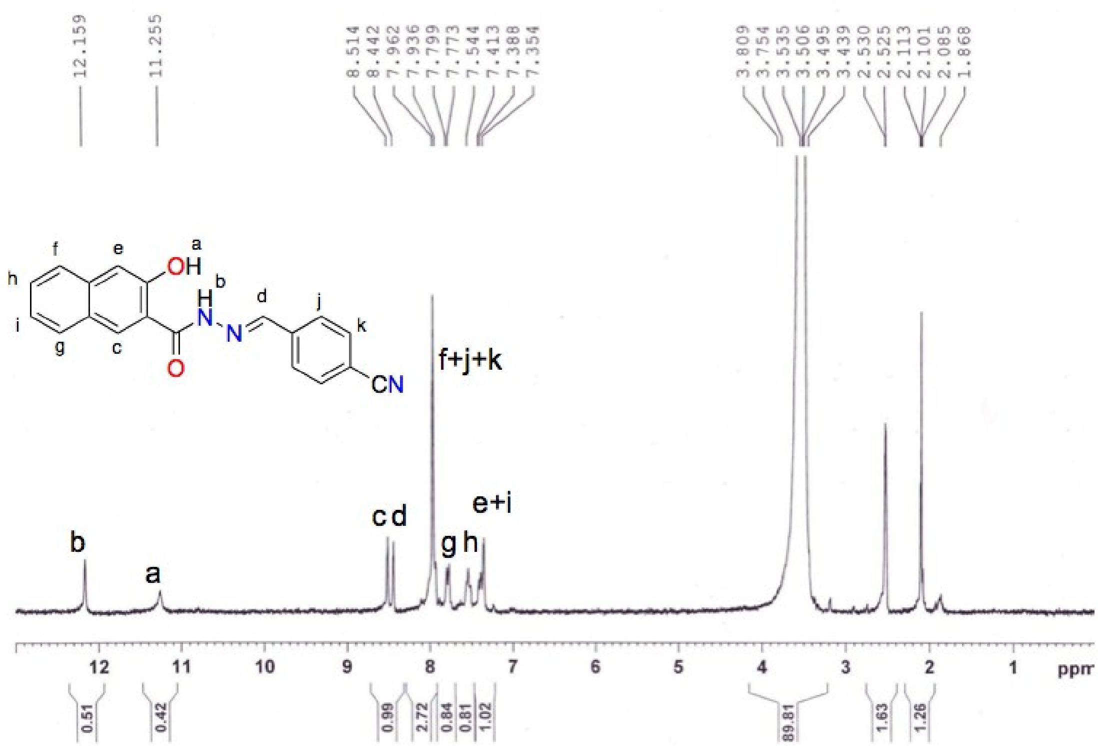

Figure S1. ^{1}H NMR (300 MHz) spectrum of **HNHCB** in d_6-DMSO at 20 ºC

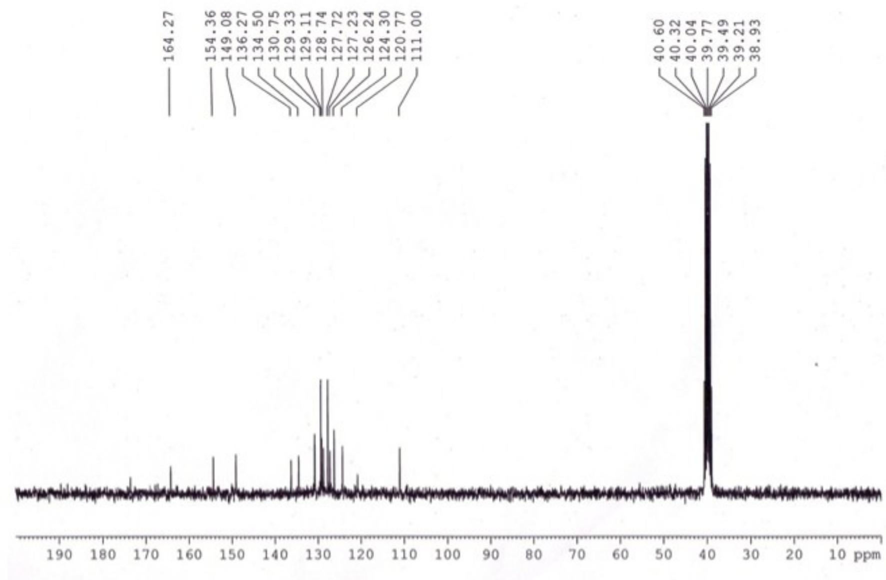

Figure S2. ^{13}C NMR (300 MHz) spectrum of **HNHCB** in d_6-DMSO at 20 ºC

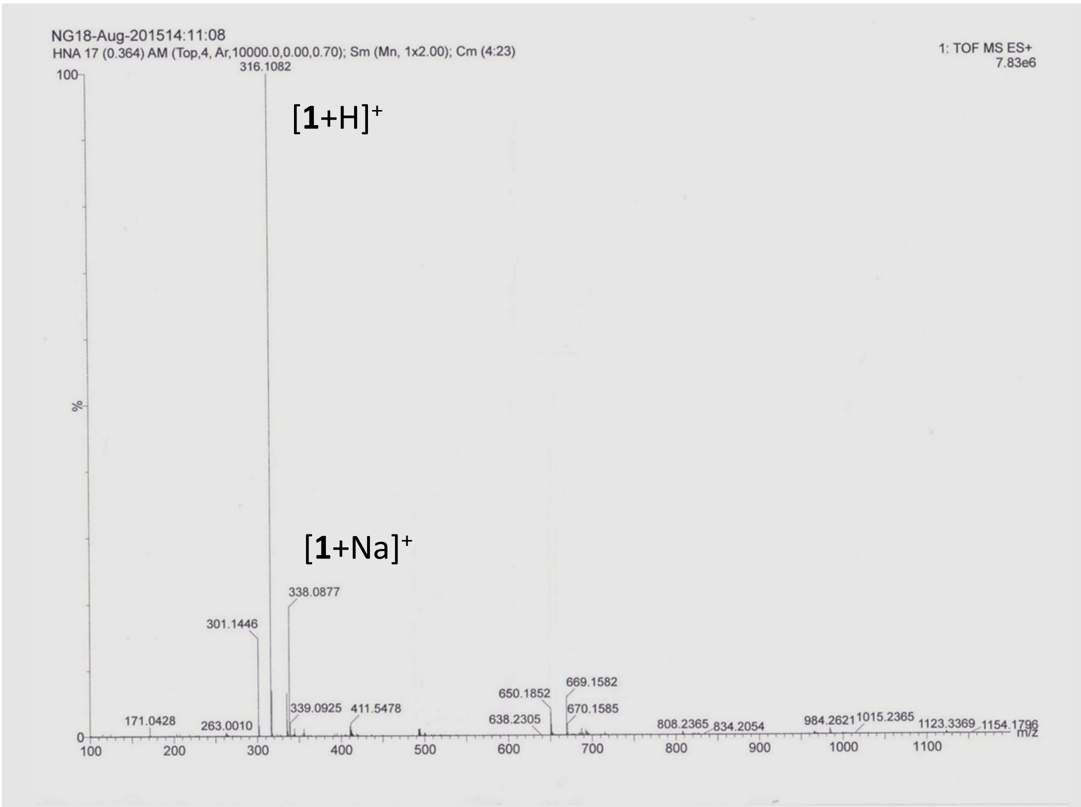

Fig. S3. Mass spectra (TOF-MS ES+) of **HNHCB**

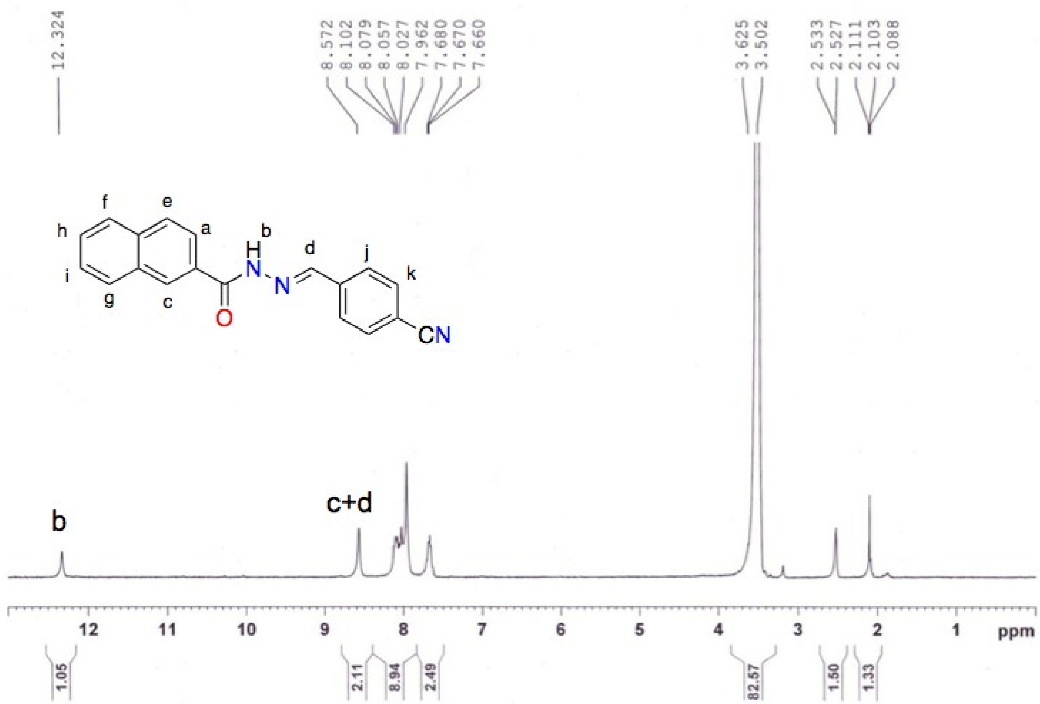

Figure S4. ^{1}H NMR (300 MHz) spectrum of **NHCB** in d_6-DMSO at 20 ºC

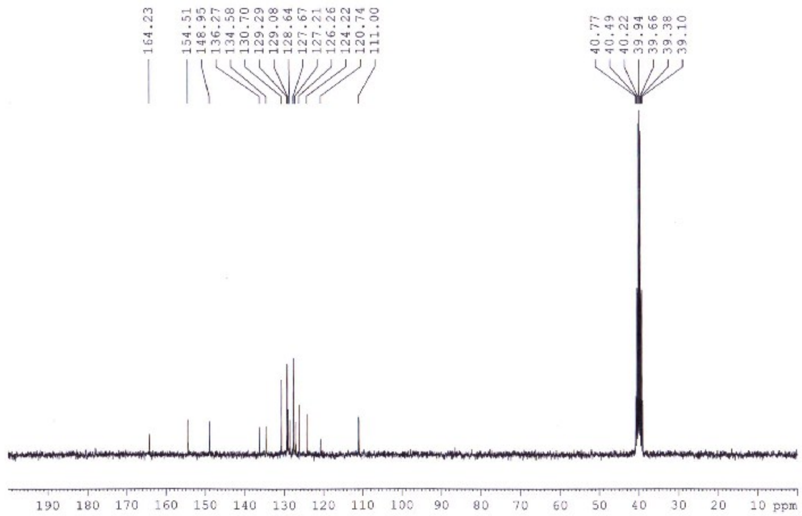

Figure S5. ^{13}C NMR (300 MHz) spectrum of **NHCB** in d_6-DMSO at 20 ºC

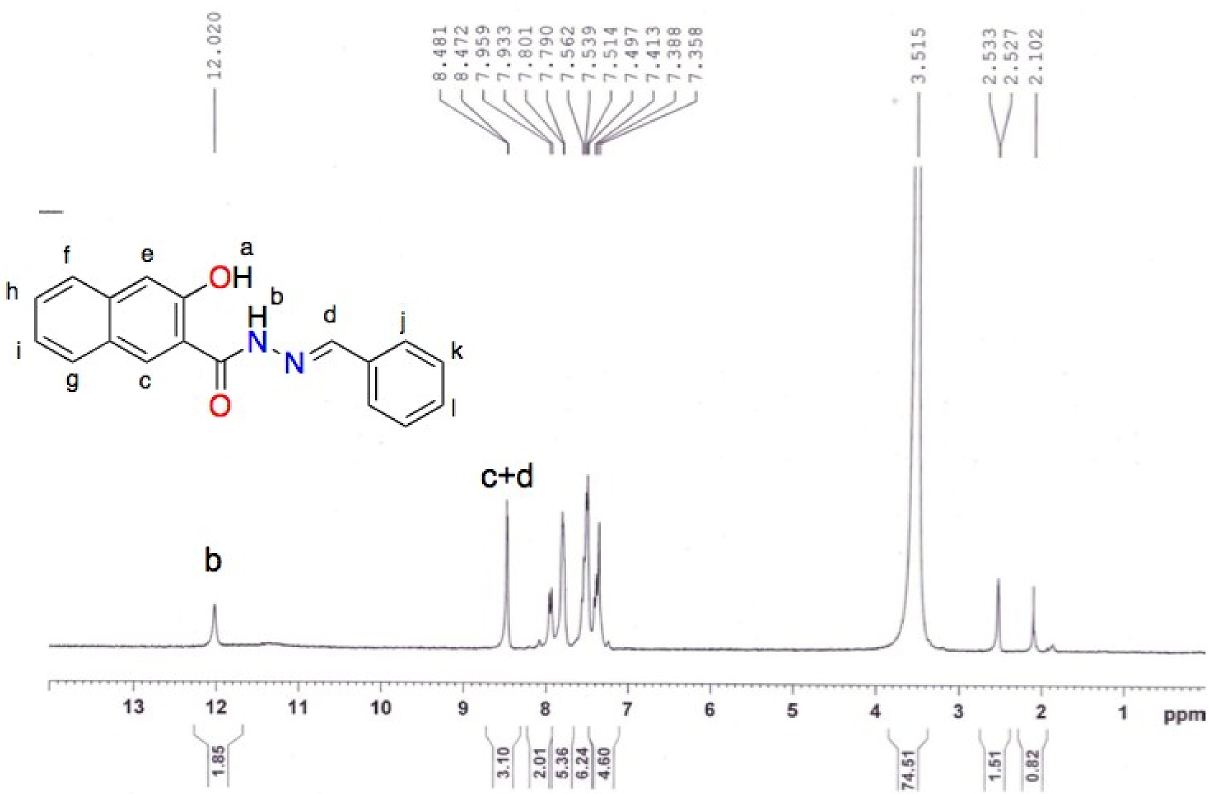

Figure S6. [1]H NMR (300 MHz) spectrum of **HNHB** in d_6-DMSO at 20 ºC

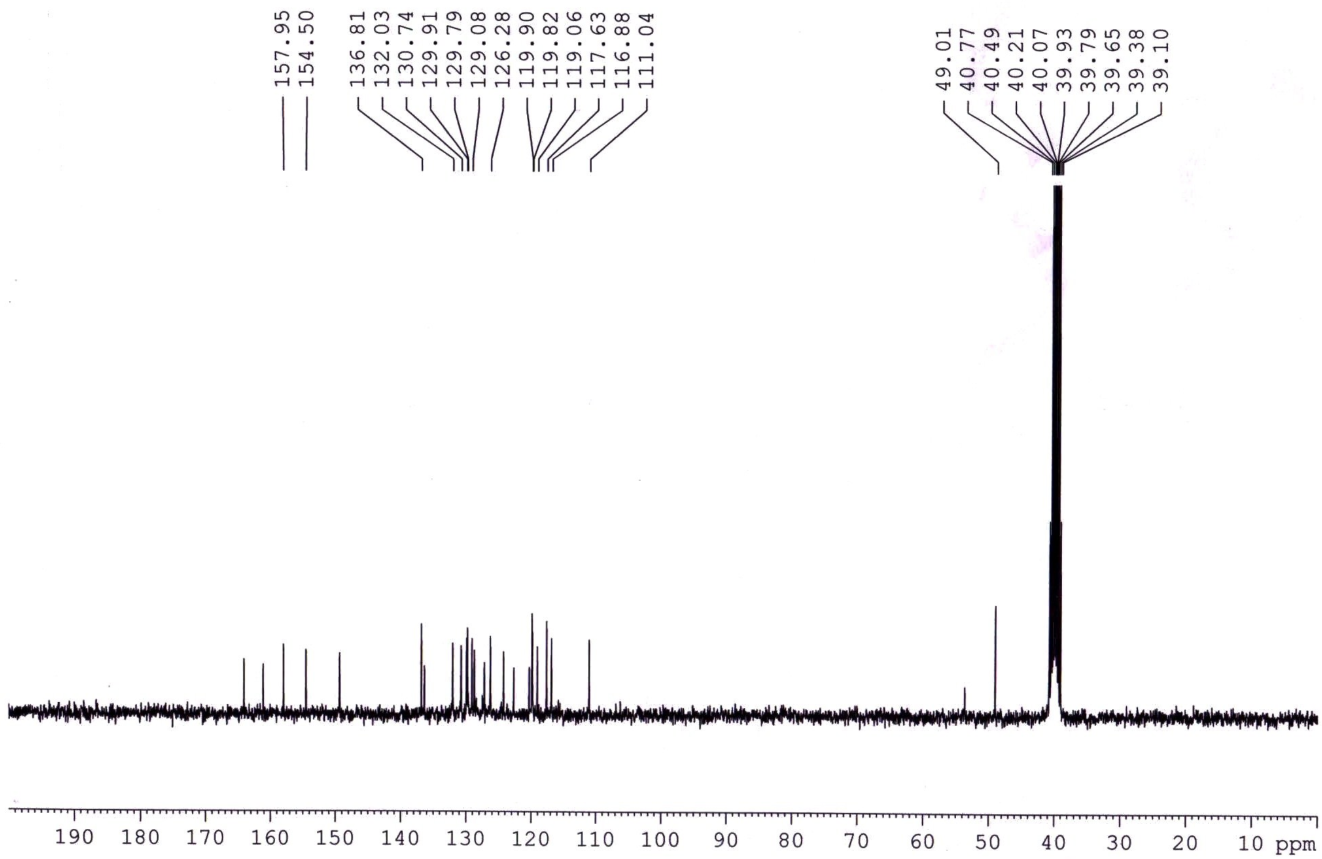

Figure S7. ^{13}C NMR (300 MHz) spectrum of **HNHB** in d_6-DMSO at 20 ºC

3. Naked-eye color change

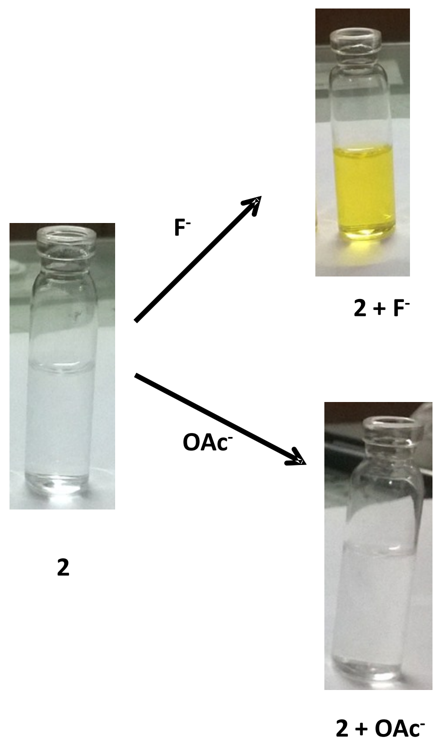

Figure S8. Naked-eye color changes of compound **2 (NHCB)** (1.0×10^{-5} M) after addition of 2 equivalent of F^- and OAc^- in acetonitrile water mixture (7:3, v/v).

4. UV–Vis Spectra

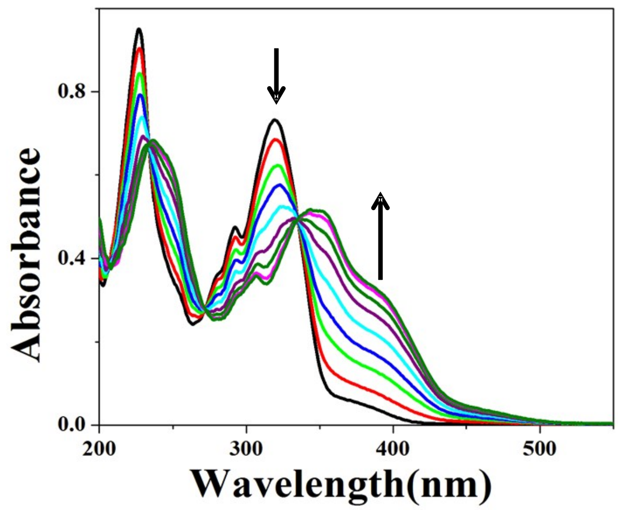

Figure S9. UV–vis spectral changes of **HNHCB** (1.0×10^{-6} M) upon addition of OAc^- ion (0–5 equiv.) in acetonitrile water mixture (7:3, v/v).

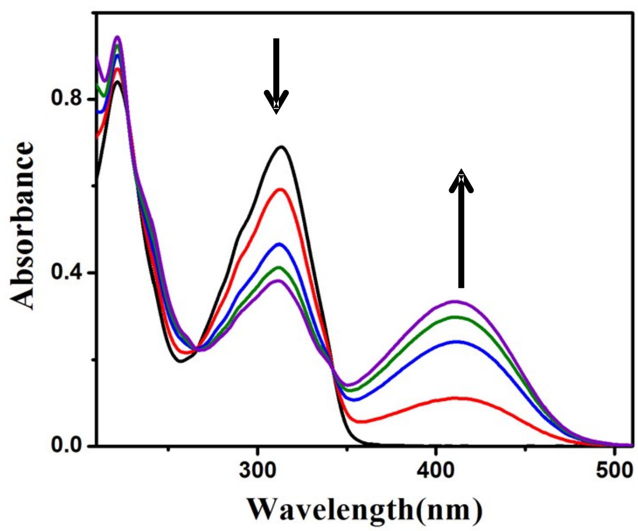

Figure S10. UV–vis spectral changes of **NHCB** (0.5 μM) in presence of F^- ion (0-2.5eqv.) in aqueous acetonitrile solvent (7:3, v/v).

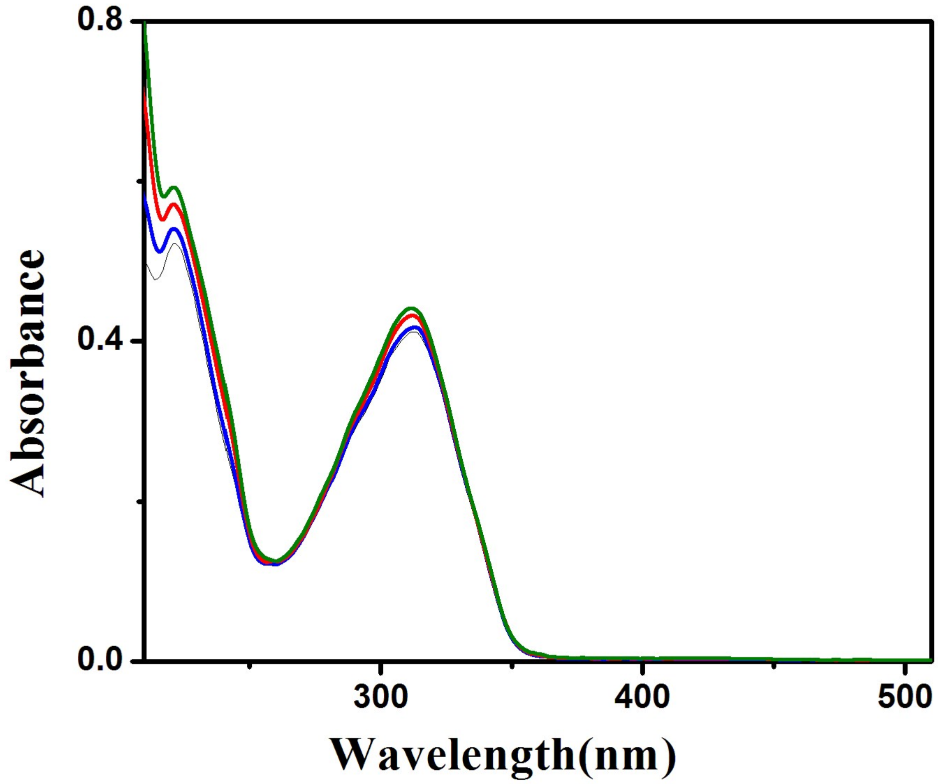

Figure S11. UV–vis spectral changes of **NHCB** (0.5 μM) in presence of AcO^- ion (0-2.5eqv.) in acetonitrile water mixture (7:3, v/v).

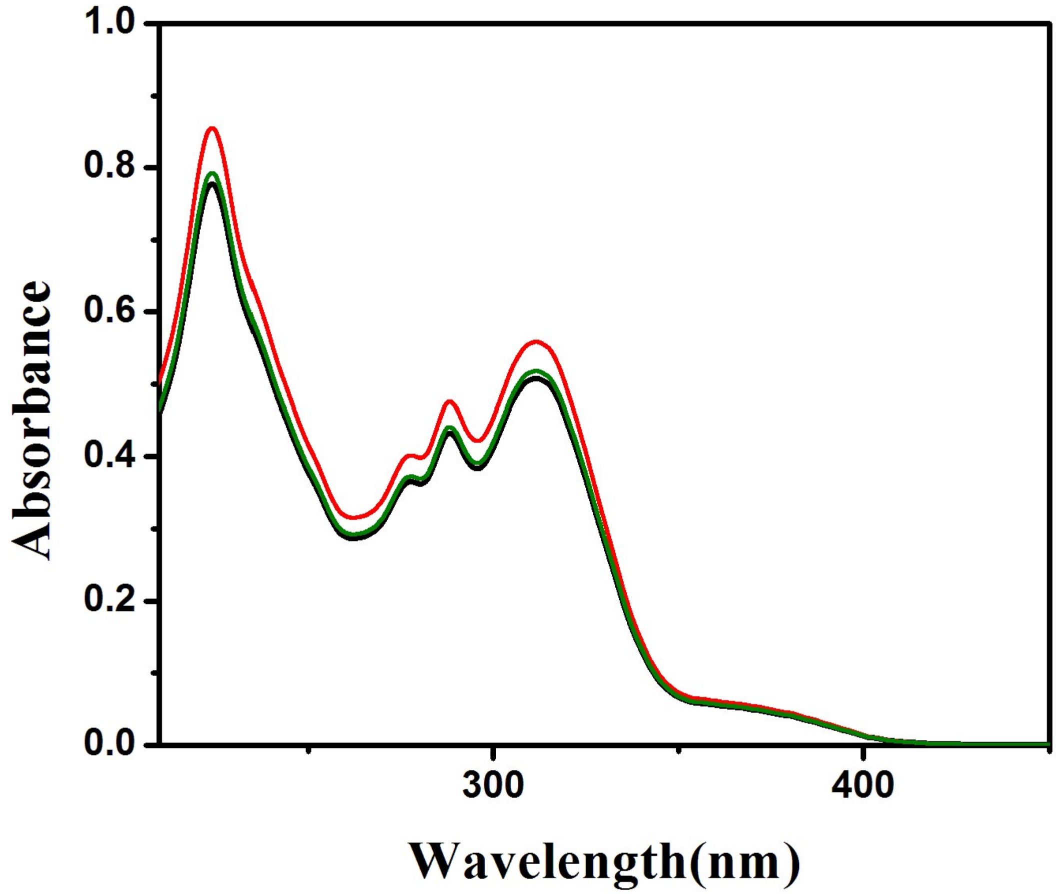

Figure S12. UV–vis spectral changes of **HNHB** (0.5 μM) in presence of F^- ion (0-2.5eqv.) in acetonitrile water mixture (7:3, v/v).

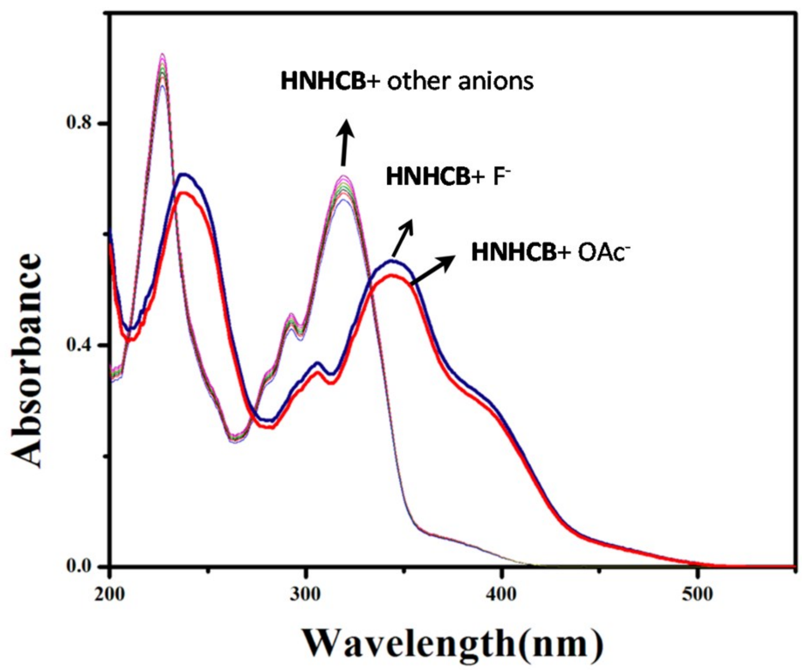

Figure S13. UV–vis spectral changes of **HNHCB** (0.5 μM) in presence of F^-, AcO^-, $H_2PO_4^-$, Cl^-, Br^-, HSO_3^-, NO_3^- and CN^- ion (0-2.5eqv.) in acetonitrile water mixture (7:3, v/v).

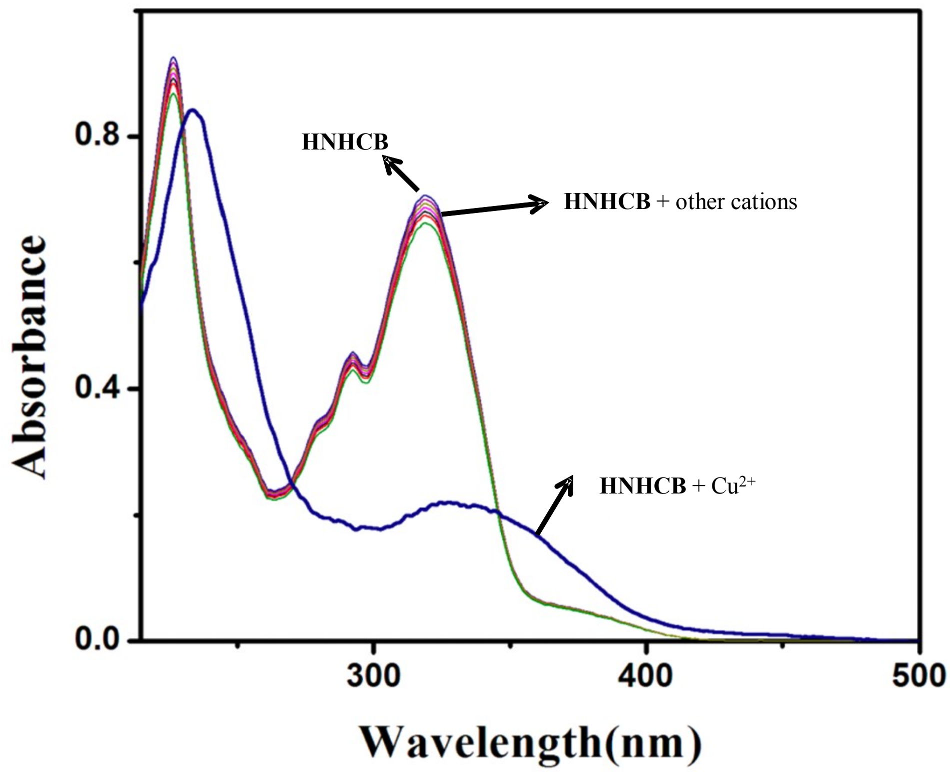

Figure S14. UV–vis spectral changes of **HNHCB** (0.5 μM) in presence of other cations (Cu^{2+}, Mn^{2+}, Fe^{2+}, Fe^{3+}, Cr^{3+}, Co^{2+}, Ni^{2+}, Zn^{2+}, Cd^{2+} , Hg^{2+} , Ca^{2+}, Mg^{2+}, Pb^{2+}ion (0-2.5eqv.) .) in acetonitrile water mixture (7:3, v/v).

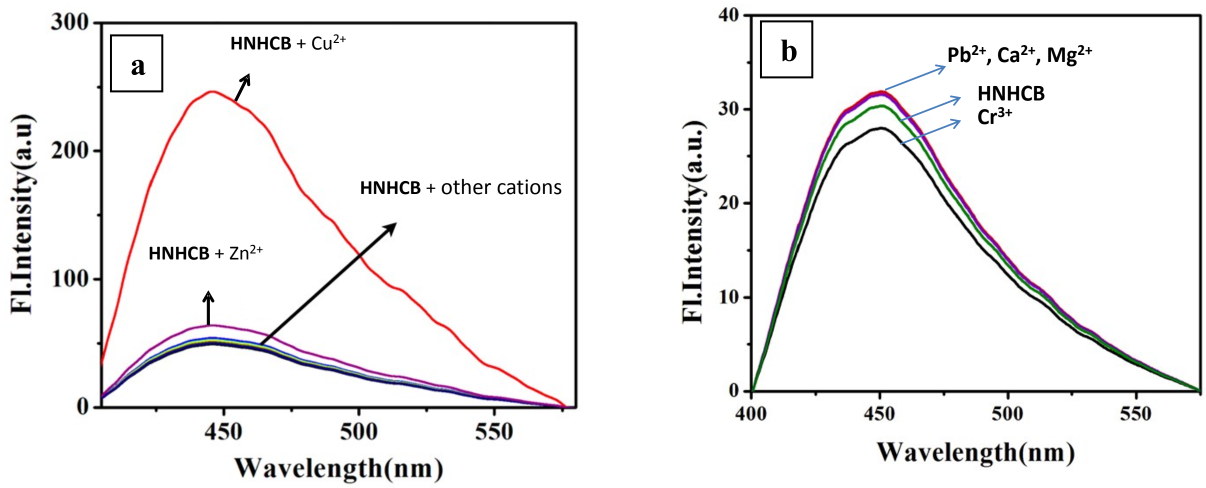

Figure S15. Emission intensity of **HNHCB** (0.5 μM) (a) in presence of Cu^{2+}, Mn^{2+}, Fe^{2+}, Fe^{3+}, Co^{2+}, Ni^{2+}, Zn^{2+}, Cd^{2+} and Hg^{2+} ion (b) in presence of Pb^{2+}, Ca^{2+}, Mg^{2+}, Cr^{3+} (0-2.5eqv.) in acetonitrile water mixture (7:3, v/v).

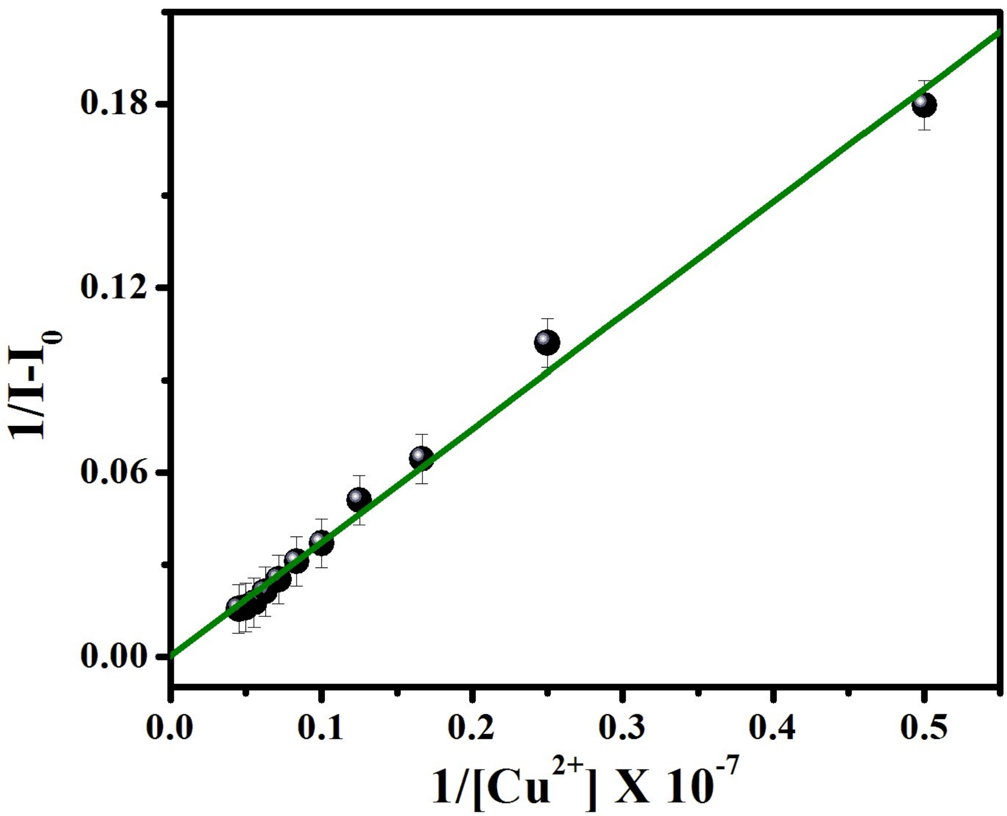

Figure S16. Benesi–Hildebrand plot for 1:1 complexation of **HNHCB** -Cu^{2+} complex

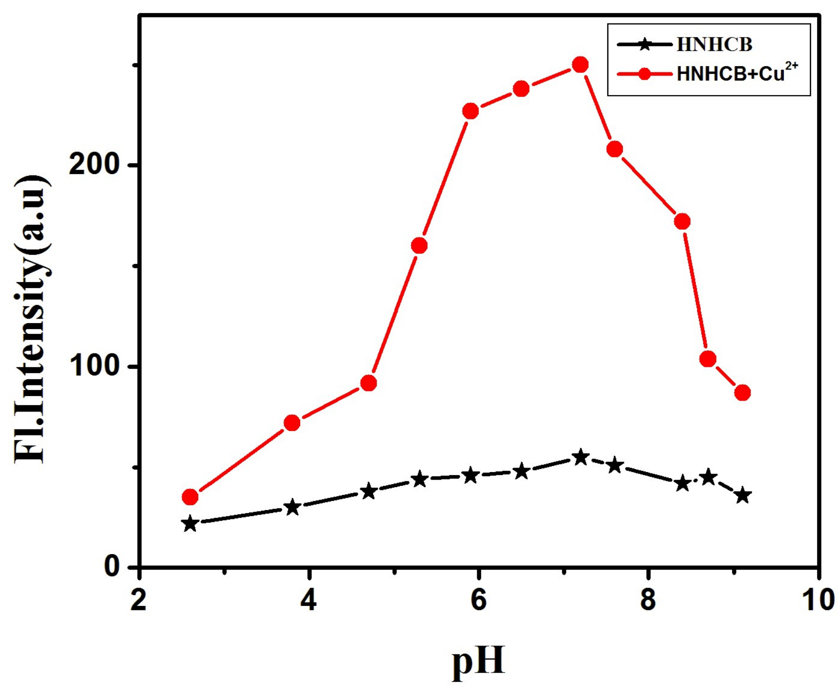

Figure S17. The fluorescence intensities of **HNHCB** and **HNHCB**–Cu^{2+} at various pH values at room temperature in acetonitrile water mixture (Tris-HCl buffer, pH = 7.2, CH_3CN–H_2O = 7 : 3, v/v)

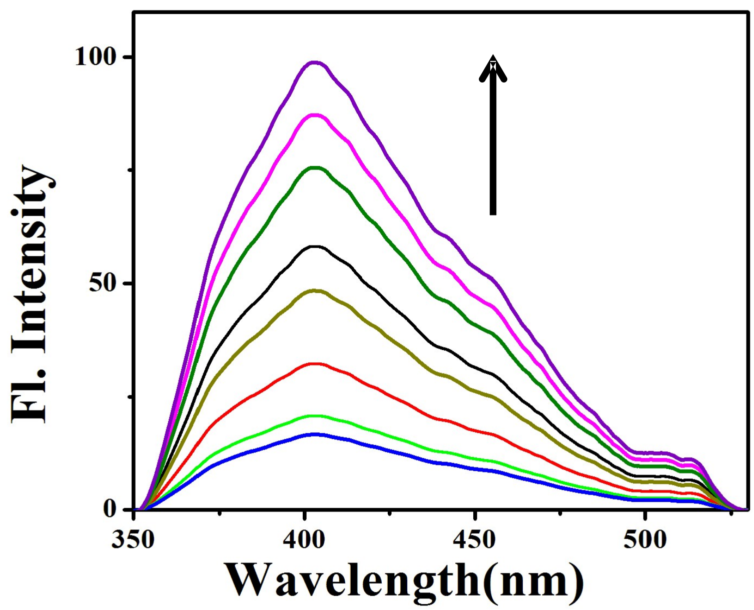

Figure S18. Emission intensity of H**NHB** (0.5 μM) in presence of Cu^{2+} (0-5eqv.) in acetonitrile water mixture (7:3, v/v).

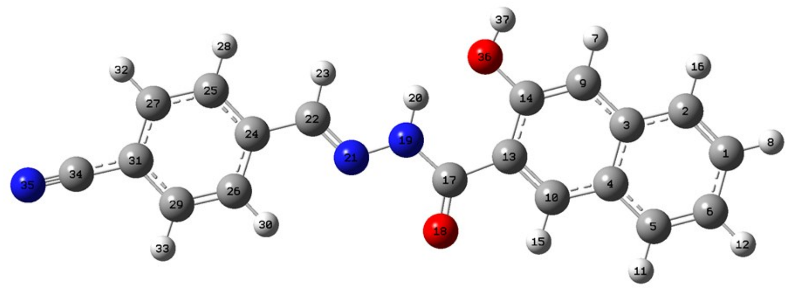

1

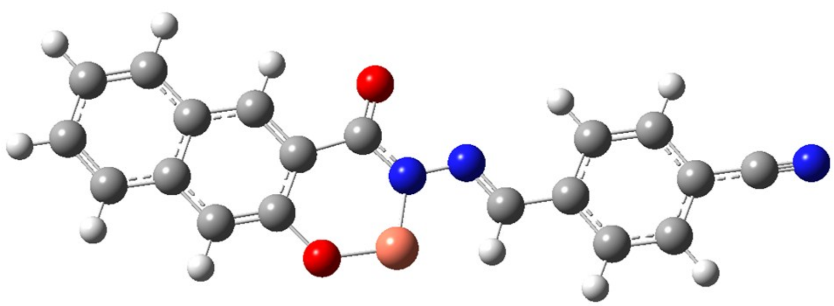

HNHCB +Cu^{2+}

Figure S19. B3LYP optimized structure of **HNHCB** (top) and **HNHCB** –Cu^{2+} complex (bottom)

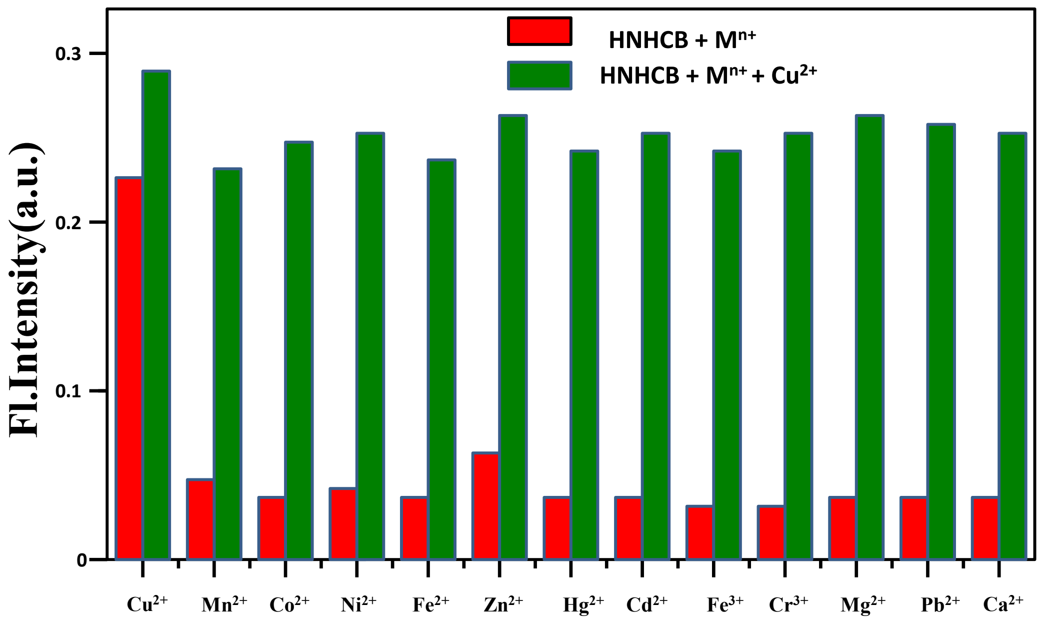

Figure S20. The selectivity of **HNHCB** for Cu^{2+} in the presence of other metal ions in acetonitrile water mixture ($CH_3CN–H_2O$ = 7 : 3, v/v), λem = 440 nm

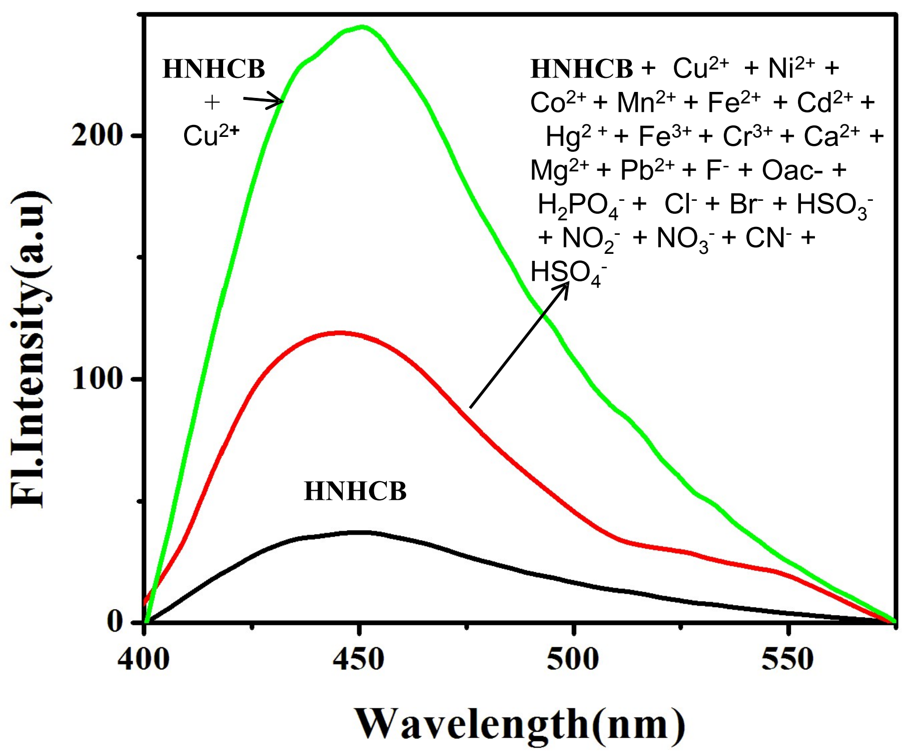

Figure S21. Fluorescence spectra of **HNHCB** (1×10^{-7} M), **HNHCB** with copper ion and **HNHCB** with mixture of ions (Cu^{2+}, Ni^{2+}, Co^{2+}, Mn^{2+}, Fe^{2+}, Cd^{2+}, Hg^{2+}, Ca^{2+}, Mg^{2+}, Pb^{2+}, Fe^{3+}, Cr^{3+}, F^-, OAc^-, $H_2PO_4^-$, Cl^- ,Br^-, NO_3^- , NO_2^-, CN^-, HSO_3^- and HSO_4^-) in acetonitrile water mixture (7:3, v/v)

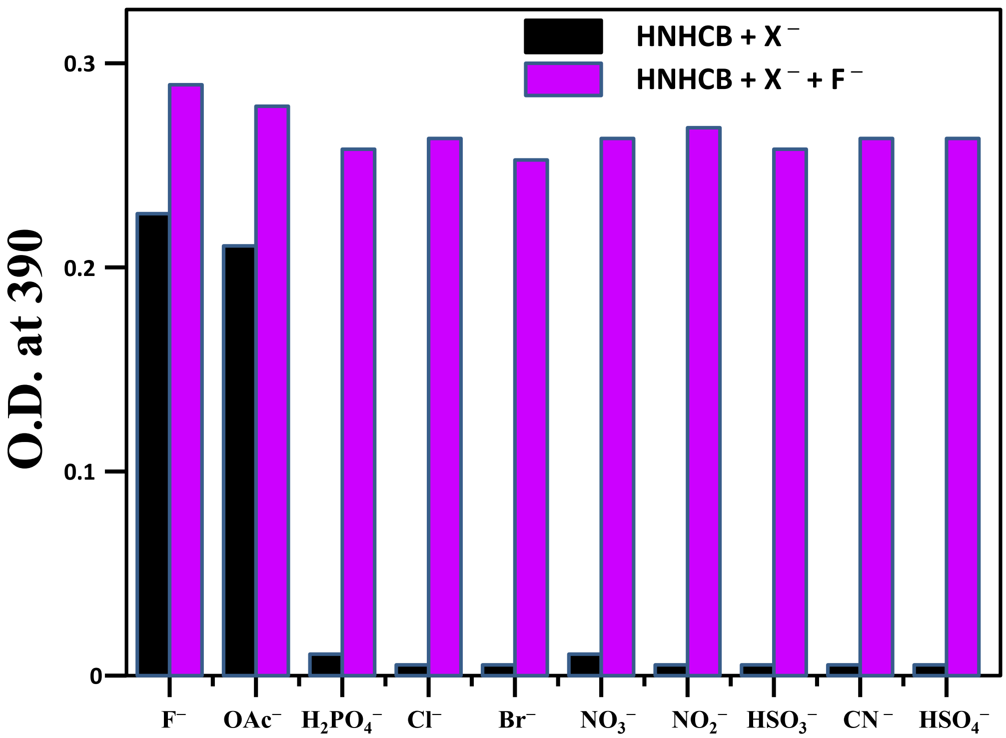

Figure S22. The selectivity of **HNHCB** for F^- in the presence of other anions in acetonitrile water mixture ($CH_3CN–H_2O$ = 7 : 3, v/v)

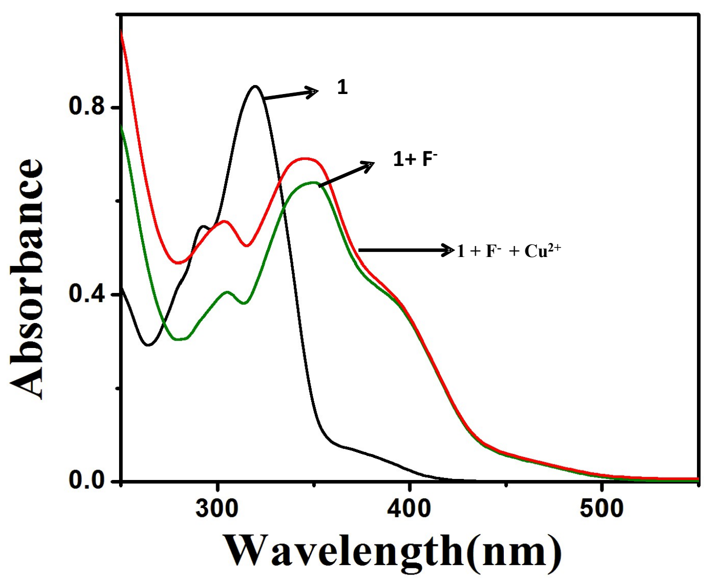

Figure S23. UV–vis spectral changes of **1(HNHCB)** in bare $F^-$and in presence of F^- and Cu^{2+} mixture in aqueous acetonitrile (7:3, v/v).

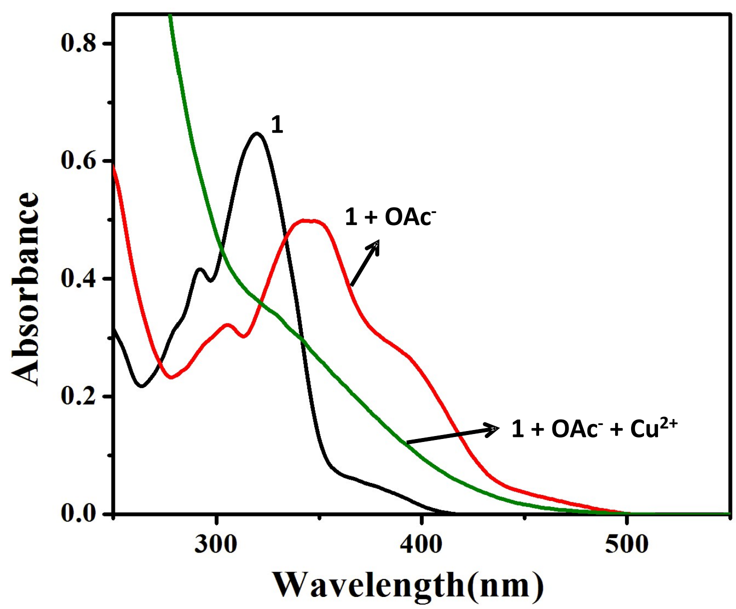

Figure S24. UV–vis spectral changes of **1(HNHCB)** in bare OAc $^{-}$and in presence of OAc^{-} and Cu^{2+} mixture in aqueous acetonitrile (7:3, v/v).

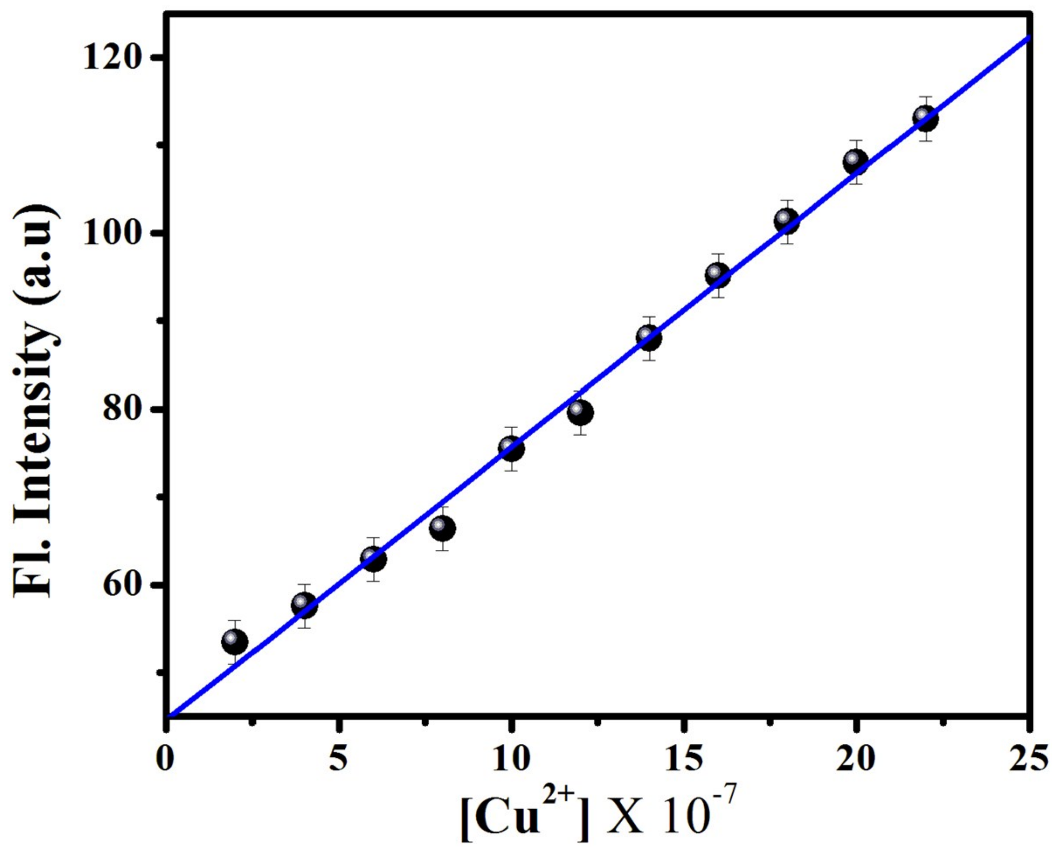

Figure S25. Determination of detection limit of Cu^{2+} by **HNHCB** (1× 10^{-7}) in CH_3CN-water mixture at λ_{em} = 443nm.

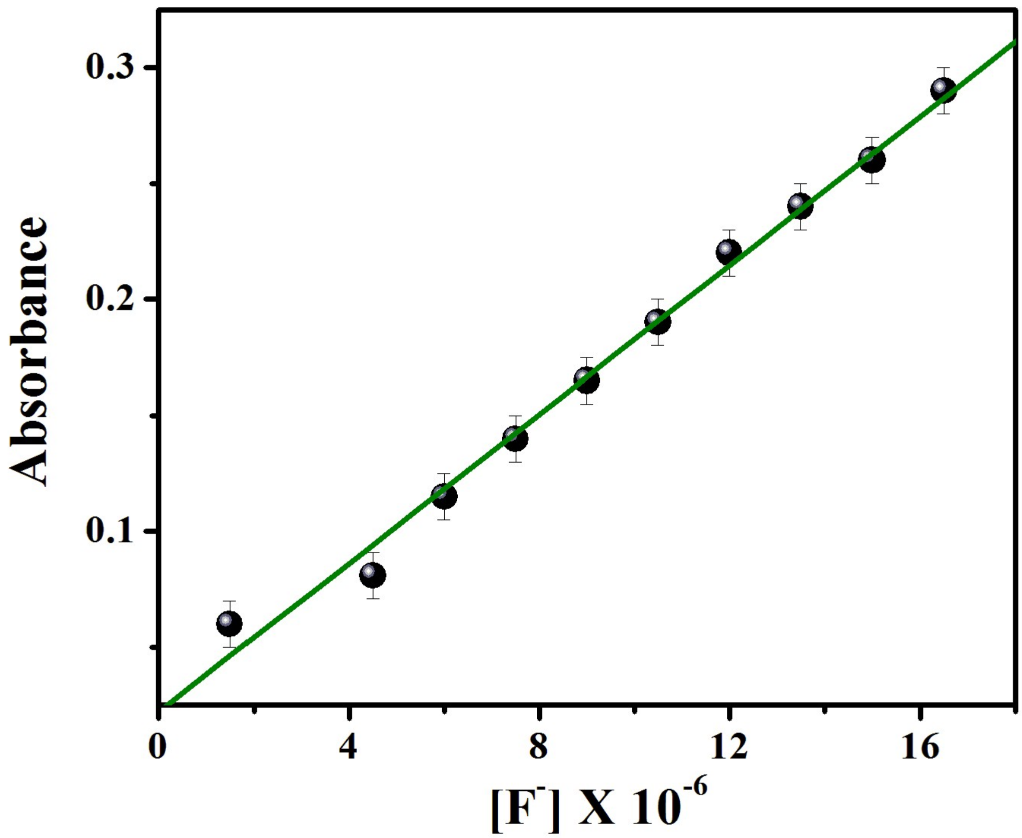

Figure S26. Determination of detection limit of F^- by **HNHCB** (1x 10^{-6}) in water acetonitrile mixture at λ_{abs} =390nm.

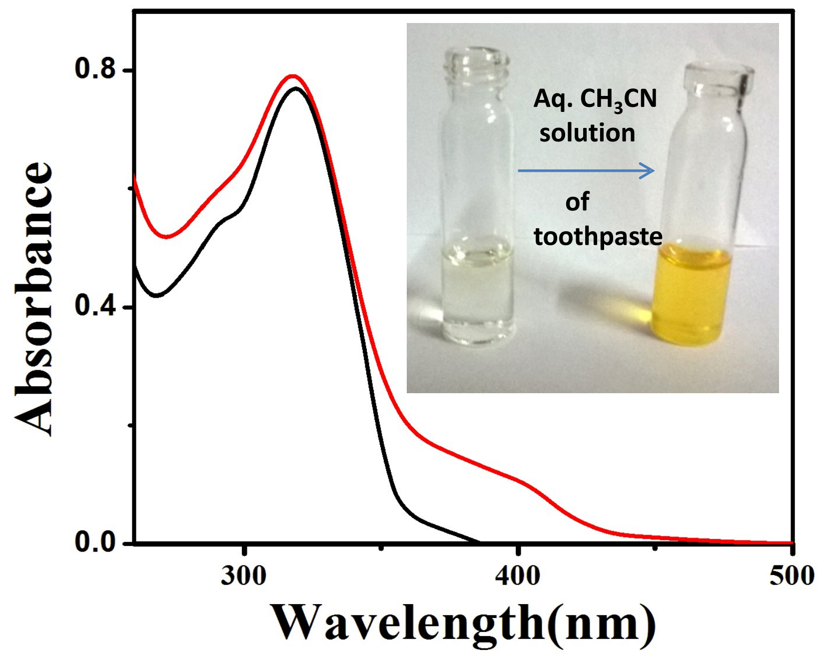

Fig. S27 Uv-vis spectra of **HNHCB** (1×10^{-5} M) and **HNHCB** in presence of toothpaste in aqueous acetonitrile solution and Naked-eye color change (inset).

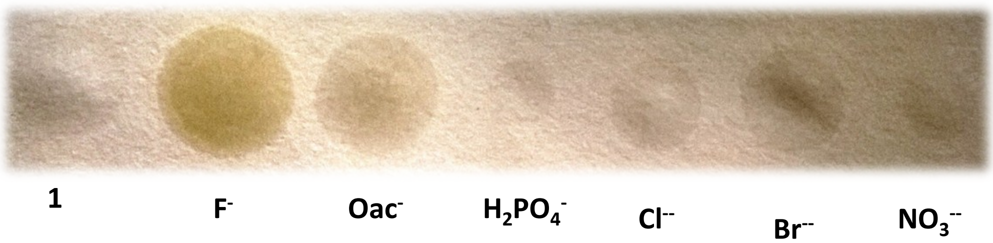

Fig. S28 Color change of test paper containing **HNHCB** (10^{-4} M) in presence of different anions

Table S1. Some useful data calculated from fluorescence decay behavior of **HNHCB** and its complexes with Cu^{2+}

Environment	r_1^b(ns)	r_2^b(ns)	r_3^b(ns)	α_1	α_2	α_3	τ_{av} (ns)	χ^2
CH_3CN-H_2O	0.06695	0.66899	5.44898	0.73	0.24	0.019	0.32	1.003
Cu(II)	0.124558	0.68152	4.85526	0.87	0.10	0.012	0.34	0.998

Table S2. Some useful theoretical parameters of **HNHCB** and after complexation with Cu^{2+}

Substrates	C14-O36	C17-N19	C17…O18	C22…N21	N19-N21	O36-H37	O-Cu^{2+}	N-Cu^{2+}
1	1.377	1.387	1.219	1.286	1.350	0.966	-	-
1+Cu^{2+}	1.415	1.324	1.22	1.286	1.350		1.70	1.651

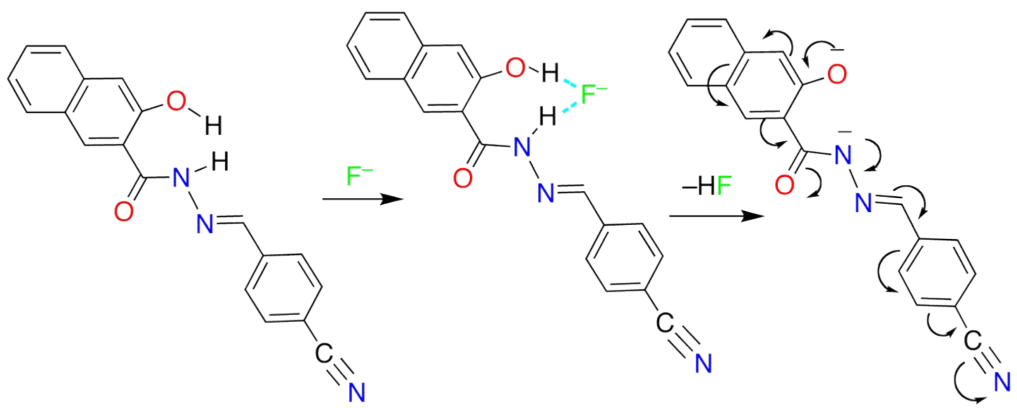

Scheme S2. Plausable mechanism of color change of **HNHCB** in presence of F^-